Low-Rate TCP-Targeted Denial of Service Attacks and Counter Strategies

Aleksandar Kuzmanovic and Edward W. Knightly

Abstract—**Denial of Service attacks are presenting an increasing threat to the global inter-networking infrastructure. While TCP's congestion control algorithm is highly robust to diverse network conditions, its implicit assumption of end-system cooperation results in a well-known vulnerability to attack by high-rate non-responsive flows. In this paper, we investigate a class of *low-rate* denial of service attacks which, unlike high-rate attacks, are difficult for routers and counter-DoS mechanisms to detect. Using a combination of analytical modeling, simulations, and Internet experiments, we show that maliciously chosen low-rate DoS traffic patterns that exploit TCP's retransmission timeout mechanism can throttle TCP flows to a small fraction of their ideal rate while eluding detection. Moreover, as such attacks exploit protocol homogeneity, we study fundamental limits of the ability of a class of randomized timeout mechanisms to thwart such low-rate DoS attacks.**

Keywords—**Denial of Service, TCP, retransmission timeout**

I. Introduction

Denial of Service (DoS) attacks consume resources in networks, server clusters, or end hosts, with the malicious objective of preventing or severely degrading service to legitimate users. Resources that are typically consumed in such attacks include network bandwidth, server or router CPU cycles, server interrupt processing capacity, and specific protocol data structures. Example DoS attacks include TCP SYN attacks that consume protocol data structures on the server operating system; ICMP directed broadcasts that direct a broadcast address to send a flood of ICMP replies to a target host thereby overwhelming it; and DNS flood attacks that use specific weaknesses in DNS protocols to generate high volumes of traffic directed at a targeted victim.

Common to the above attacks is a large number of compromised machines or agents involved in the attack and a "sledgehammer" approach of high-rate transmission of packets toward the attacked node. While potentially quite harmful, the high-rate nature of such attacks presents a statistical anomaly to network monitors such that the attack can potentially be detected, the attacker identified, and the effects of the attack mitigated (see for example, [8], [26], [34]).

In this paper, we study low-rate DoS attacks, which we term "shrew attacks,"[1] that attempt to deny bandwidth to TCP flows while sending at sufficiently low average rate to elude detection by counter-DoS mechanisms.

TCP congestion control operates on two time-scales. On smaller time-scales of round trip times (RTT), typically 10's to 100's of msec, TCP performs additive-increase multiplicative-decrease (AIMD) control with the objective of having each flow transmit at the fair rate of its bottleneck link. At times of severe congestion in which multiple losses occur, TCP operates on longer time-scales of Retransmission Time Out (RTO).[2] In an attempt to avoid congestion collapse, flows reduce their congestion window to one packet and wait for a period of RTO after which the packet is resent. Upon further loss, RTO doubles with each subsequent timeout. If a packet is successfully received, TCP re-enters AIMD via slow start.

To explore low-rate DoS, we take a frequency-domain perspective and consider periodic on-off "square-wave" shrew attacks that consist of short, maliciously-chosen-duration bursts that repeat with a fixed, maliciously chosen, slow-time-scale frequency. Considering first a single TCP flow, if the total traffic (DoS and TCP traffic) during an RTT-time-scale burst is sufficient to induce enough packet losses, the TCP flow will enter a timeout and attempt to send a new packet RTO seconds later. If the period of the DoS flow approximates the RTO of the TCP flow, the TCP flow will continually incur loss as it tries to exit the timeout state, fail to exit timeout, and obtain near zero throughput. Moreover, if the DoS period is near but outside the RTO range, significant, but not complete throughput degradation will occur. Hence the foundation of the shrew attack is a null frequency at the relatively slow time-scale of approximately RTO enabling a low average rate attack that is difficult to detect.

In a simplified model with heterogeneous-RTT aggregated flows sharing a bottleneck link, we derive an expression for the throughput of the attacked flows as a function of the time-scale of the DoS flow, and hence of the DoS flow's average rate. Furthermore, we derive the "optimal" DoS traffic pattern (a two-level periodic square wave) that minimizes its average rate for a given level of TCP throughput for the victim, including zero throughput.

Next, we use *ns* simulations to explore the impact of aggregation and heterogeneity on the effectiveness of the shrew attack. We show that even under aggregate flows with heterogeneous RTT's, heterogeneous file sizes, different TCP variants (New Reno, Sack, etc.), and different buffer management schemes (drop tail, RED, etc.), similar behavior occurs albeit with different severity for different flows and scenarios. The reason for this is that once the first brief outage occurs, all flows will simultaneously timeout. If their RTOs are nearly identical, they synchronize to the attacker's period and will enter a cycle identical to the single-flow case, even with heterogeneous RTTs and aggregation. However, with highly variable RTTs, the success of the shrew attack is weighted such that small RTT flows will degrade far worse than large RTT flows, so that the attack has the effect of a high-RTT-pass filter. We show that in all such cases,

A. Kuzmanovic is with the EECS Department at Northwestern University. E. Knightly is with the ECE/CS Departments at Rice University.

This research is supported by the National Science Foundation.

A subset of this work appears in the Proceedings of ACM Sigcomm '03 [22].

[1] A shrew is a small but aggressive mammal that ferociously attacks and kills much larger animals with a venomous bite.

[2] recommended minimum value 1 sec [2]

detection mechanisms for throttling non-responsive flows such as RED-PD or CHOKe are not able to throttle the DoS attacker.

We then perform a set of Internet experiments in both a local and wide area environment. While necessarily small scale experiments (given that the expected outcome is to reduce TCP throughput to near zero), the experiments validate the basic findings and show that even a remote attacker (across a WAN) can dramatically reduce TCP throughput. For example, in the WAN experiments, a remote 909 kb/sec average-rate attack consisting of 100 ms bursts at the victim's RTO time-scale reduced the victim's throughput from 9.8 Mb/sec to 1.2 Mb/sec.

Finally, we explore potential solutions to shrew attacks. First, we explore an approach where we increase the initial TCP window size in an attempt to help TCP flows to survive attacker-induced outages. Second, while it may appear attractive to remove the RTO mechanism all together or choose very small RTO values, we do not pursue this avenue as timeout mechanisms are fundamentally required to achieve high performance during periods of heavy congestion [2]. Instead, we consider a class of randomization techniques in which flows randomly select a value of minRTO such that they have random null frequencies. We use a combination of analytical modeling and simulation to show that such strategies can only distort and slightly mitigate TCP's frequency response to the shrew attack. Moreover, we devise an optimal DoS attack given that flows are randomizing their RTOs and show that such an attack is still quite severe.

In summary, vulnerability to low-rate DoS attacks is not a consequence of poor or easily fixed TCP design, as TCP necessarily requires congestion control mechanisms at both fast (RTT) and slow (RTO) time-scales to achieve high performance and robustness to diverse network conditions. Consequently, it appears that such attacks can only be mitigated and not prevented through randomization. Development of prevention mechanisms that detect malicious low-rate flows remains an important area for future research.

The reminder of this paper is organized as follows. In Section II we present background on TCP's timeout mechanism, while in Section III we explain and model the origins of the vulnerability of the timeout mechanism to low-rate attacks. Next, in Section IV, we explore the traffic patterns to perform the attacks, while in Section V we explore the impact of TCP flow aggregation and heterogeneity on the effectiveness of the shrew attack. Section VI describes the experiments performed in the Internet, and Section VII proposes and evaluates a set of core- and end-point-based counter-DoS mechanisms intended to mitigate the effects of shrew attacks. Finally, in Section VIII we conclude.

II. TCP's Timeout Mechanism

Here, we present background on TCP's retransmission timeout (RTO) mechanism [32]. TCP detects loss via either timeout from non-receipt of ACKs, or by receipt of a triple-duplicate ACK. If loss occurs and less than three duplicate ACKs are received, TCP waits for a period of retransmission timeout to expire, reduces its congestion window to one packet and resends the packet.[3]

Selection of the timeout value requires a balance among two extremes: if set too low, spurious retransmissions will occur when packets are incorrectly assumed lost when in fact the data or ACKs are merely delayed. Similarly, if set too high, flows will wait unnecessarily long to infer and recover from congestion.

To address the former factor, Allman and Paxson experimentally showed that TCP achieves near-maximal throughput if there exists a lower bound for RTO of one second [2]. While potentially conservative for small-RTT flows, the study found that *all flows* should have a timeout value of at least 1 second in order to ensure that congestion is cleared, thereby achieving the best performance.

To address the latter factor, a TCP sender maintains two state variables, SRTT (smoothed round-trip time) and RTTVAR (round-trip time variation). According to [32], the rules governing the computation of SRTT, RTTVAR, and RTO are as follows. Until a RTT measurement has been made for a packet sent between the sender and receiver, the sender sets RTO to three seconds. When the first RTT measurement R' is made, the host sets SRTT $=$ R', RTTVAR $=$ R'$/2$ and RTO $=$ SRTT $+ \max(\mathrm{G}, 4\mathrm{RTTVAR})$, where G denotes the clock granularity (typically ≤ 100 ms). When a subsequent RTT measurement R' is made, a host sets

$$RTTVAR = (1-\beta)\, RTTVAR + \beta\, |SRTT - R'|$$

and

$$SRTT = (1-\alpha) SRTT + \alpha\, R'$$

where $\alpha = 1/8$ and $\beta = 1/4$, as recommended in [17].

Thus, combining the two parts, a TCP sender sets its value of RTO according to

$$RTO = \max(minRTO,\, SRTT + \max(G, 4\, RTTVAR)). \quad (1)$$

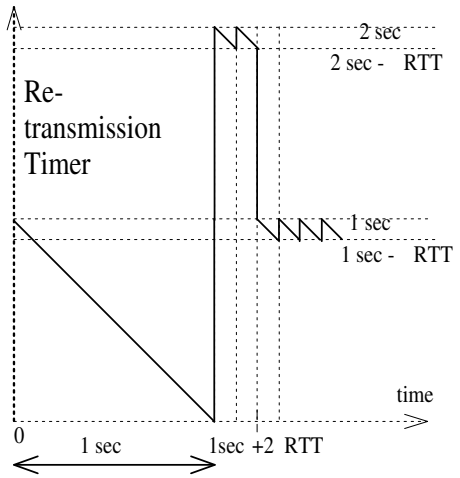

Fig. 1. Behavior of the TCP retransmission timer

Finally, we illustrate RTO management via a *retransmission-timer* timeline in Figure 1. Assume that a packet with sequence

[3]Conditions under which TCP enters retransmission timeout vary slightly according to TCP version. We discuss this issue in Section V.

number n is sent by a TCP sender at reference time $t = 0$, and that a retransmission timer of 1 second is initiated upon its transmission. If packet n is lost and fewer than three duplicate ACKs are received by the sender, the flow "times out" when the timer expires at $t = 1$ sec. At this moment, the sender enters the exponential backoff phase: it reduces the congestion window to one, doubles the RTO value to 2 seconds according to Karn's algorithm [21], retransmits the unacknowledged packet with sequence number *n*, and resets the retransmission timer with this new RTO value. If the packet is lost again (*not* shown in Figure 1), exponential backoff continues as the sender waits for the 2 sec-long retransmission timer to expire. At $t = 3$ sec, the sender again applies Karn's algorithm, doubles the RTO value to 4 seconds and repeats the process.

Alternately, if packet *n* is successfully retransmitted at time $t = 1$ sec as illustrated in Figure 1, its ACK will arrive to the sender at time $t = 1 + \text{RTT}$. At this time, the TCP sender exits the exponential backoff phase and enters slow start, doubling the window size to two, transmitting two new packets $n + 1$ and $n + 2$, and resetting the retransmission timer with the current RTO value of 2 sec. If the two packets are not lost, they are acknowledged at time $t = 1 + 2\,\text{RTT}$, and SRTT, RTTVAR and RTO are recomputed as described above. Provided that $\text{minRTO} > \text{SRTT} + \max(\text{G}, 4\,\text{RTTVAR})$, RTO is again set to 1 sec. Thus, in this scenario in which timeouts occur but exponential backoff does not, the value of RTO deviates by no more than RTT from minRTO for $t > \text{minRTO} + 2$ RTT.

III. DoS Origins and Modeling

In this section, we describe how an attacker can exploit TCP's timeout mechanism to perform a DoS attack. Next, we provide a scenario and a system model of such an attack. Finally, we develop a simple model for aggregate TCP throughput as a function of the DoS traffic parameters.

A. Origins

The above timeout mechanism, while essential for robust congestion control, provides an opportunity for low-rate DoS attacks that exploit the slow-time-scale dynamics of retransmission timers. In particular, an attacker can provoke a TCP flow to repeatedly enter a retransmission timeout state by sending high-rate, but short-duration bursts having RTT-scale burst length, and repeating periodically at slower RTO time-scales. The victim will be throttled to near-zero throughput while the attacker will have low average rate making it difficult for counter-DoS mechanisms to detect.

We refer to the short durations of the attacker's loss-inducing bursts as *outages*, and present a simple but illustrative model relating the outage time-scale (and hence attacker's average rate) to the victim's throughput as follows.

First, consider a single TCP flow and a single DoS stream. Assume that an attacker creates an initial outage at time 0 via a short-duration high-rate burst. As shown in Figure 1, the TCP sender will wait for a retransmission timer of 1 sec to expire and will then double its RTO. If the attacker creates a second outage between time 1 and $1 + 2\,\text{RTT}$, it will force TCP to wait another 2 sec. By creating similar outages at times 3, 7, 15, $\cdots$, an attacker could exploit Karn's algorithm and deny service to the TCP flow while transmitting at extremely low average rate.

While potentially effective for a single flow, a DoS attack on TCP aggregates in which flows continually arrive and depart requires periodic (vs. exponentially spaced) outages at the minRTO time-scale. Moreover, if all flows have an identical minRTO parameter as recommended in RFC 2988 [32], the TCP flows can be forced into continual timeouts if an attacker creates periodic outages.

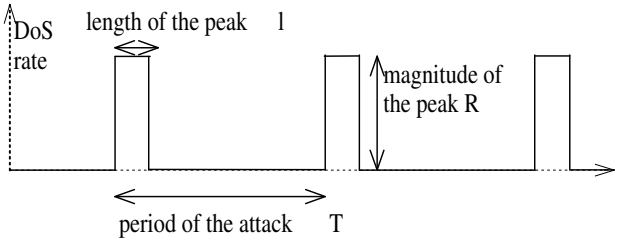

Fig. 2. Square-wave DoS stream

Thus, we consider "square wave" shrew attacks as shown in Figure 2 in which the attacker transmits bursts of duration l and rate R in a deterministic on-off pattern that has period T. As explored below, a successful shrew attack will have rate R large enough to induce loss (i.e., R aggregated with existing traffic must exceed the link capacity), duration l of scale RTT (long enough to induce timeout but short enough to avoid detection), and period T of scale RTO (chosen such that when flows attempt to exit timeout, they are faced with another loss).

B. Model

Consider a scenario of an attack shown in Figure 3(a). It consists of a single bottleneck queue driven by n long-lived TCP flows with heterogeneous RTTs and a single DoS flow. Denote RTT_i as the roundtrip time of the i-th TCP flow, $i = 1, \cdots, n$. The DoS flow is a periodic square-wave DoS stream shown in Figure 2. The following result relates the throughput of the TCP flows to the period of the attack.

DoS TCP Throughput Result. *Consider a periodic DoS attack with period T. If the outage duration satisfies*

(C1) $l' \geq RTT_i$

and the minimum RTO satisfies

(C2) $minRTO > SRTT_i + 4\,RTTVAR_i$

for all $i = 1, \cdots, n$, then the normalized throughput of the aggregate TCP flows is approximately

$$\rho(T) = \frac{\lceil \frac{minRTO}{T} \rceil T - minRTO}{\lceil \frac{minRTO}{T} \rceil T}. \qquad (2)$$

This result is obtained as follows. As shown in Figure 3(b), the periodic l-length bursts create short l'-length outages having high packet loss.[4] If l' reaches the TCP flows' RTT time-scales, i.e., $l' \geq \text{RTT}_i$, for all $i = 1, \cdots, n$, then the congestion caused by the DoS burst lasts sufficiently long to force *all* TCP flows to simultaneously enter timeout. Moreover, if $\text{minRTO} > \text{SRTT}_i + 4\,\text{RTTVAR}_i$, for $i = 1, \cdots, n$, all TCP

[4] The relationship between l and l' is explored in Section IV.

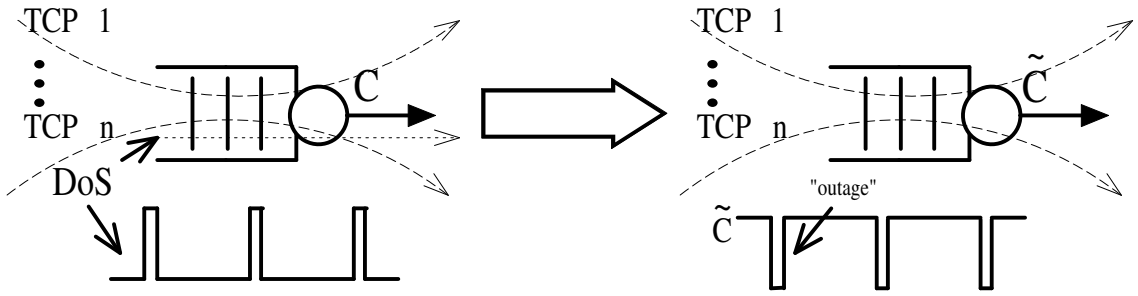

Fig. 3. DoS scenario and system model

flows will have identical values of RTO and will thus timeout after minRTO seconds, which is the ideal moment for an attacker to create a new outage. Thus, in this case, despite their heterogeneous round-trip times, all TCP flows are forced to "synchronize" to the attacker and enter timeout at (nearly) the same time, and attempt to recover at (nearly) the same time. Thus, when exposed to outages with period T, Equation (2) follows.

Equation (2) expresses the *normalized* throughput of a TCP flow under a *T*-periodic attack: a ratio of the bandwidth achievable by the TCP flow under the *T*-periodic attack, and the TCP bandwidth without any attack. For example, when $T = 1.5$ sec, and minRTO $= 1$ sec, the TCP flow utilizes the available bandwidth in the $[\text{minRTO}, T]$ period after each outage, such that the normalized TCP throughput becomes $(T - \text{minRTO})/T = 0.33$. On the other hand, when $T = 0.8$ sec, only every second outage is effective, and the TCP flow utilizes bandwidth in the $[\text{minRTO}, 2T]$ period after each effective outage in this scenario. Consequently, the normalized throughput becomes $(2T - \text{minRTO})/2T = 0.375$ according to Equation (2).

Note that Equation (2) does not model throughput losses due to the slow-start phase, but simply assumes that TCP flows utilize all available bandwidth after exiting the timeout phase. In other words, we assume that the TCP flows utilize the full link bandwidth after the end of each retransmission timeout and the beginning of the following outage. Observe that if the period T is chosen such that $T \geq 1 + 2\,\text{RTT}_i$, all TCP flows will continually enter a retransmission timeout of 1 sec duration. Thus, because Equation (2) assumes that RTO = minRTO for $T >$ minRTO, while this is not the case in the period $(\text{minRTO}, \text{minRTO} + 2\,\text{RTT})$, Equation (2) behaves as an *upper bound* in practice. In other words, periodic DoS streams are not utilizing TCP's exponential backoff mechanism but rather exploit repeated timeouts.

Next, we consider flows that do not satisfy conditions (C1) or (C2).

DoS TCP Flow-Filtering Result. *Consider a periodic DoS attack with period* T. *If the outage duration* $l' \geq$ *RTT*$_i$ *and minRTO* $>$ *SRTT*$_i + 4$ *RTTVAR*$_i$ *for* $i = 1, \cdots, k$ *whereas* $l' <$ *RTT*$_j$ *or minRTO* $\leq$ *SRTT*$_j + 4$ *RTTVAR*$_j$ *for* $j = k+1, \cdots, n$, *then Equation (2) holds for flows* $1, \cdots, k$.

This result, shown similarly to that above, states that Equation (2) holds for *any* TCP sub-aggregate for which conditions (C1) and (C2) hold. In other words, if a shrew attack is launched on a group of flows such that only a subset satisfies the two conditions, that subset will obtain degraded throughput according to Equation (2), whereas the remaining flows will not. We refer to this as "flow filtering" in that such an attack will deny service to a subset of flows while leaving the remainder unaffected, or even obtaining higher throughput. We explore this issue in detail in Section V.

C. Example

Here, we present a baseline set of experiments to explore TCP's "frequency response" to shrew attacks. We first consider the analytical model and the scenario depicted in Figure 3 in which conditions (C1) and (C2) are satisfied and minRTO $=$ 1 sec. The curve labeled "model" in Figure 4 depicts ρ vs. T as given by Equation (2). Throughput is normalized to the link capacity, which under high aggregation, is also the throughput that the TCP flows would obtain if no DoS attack were present.

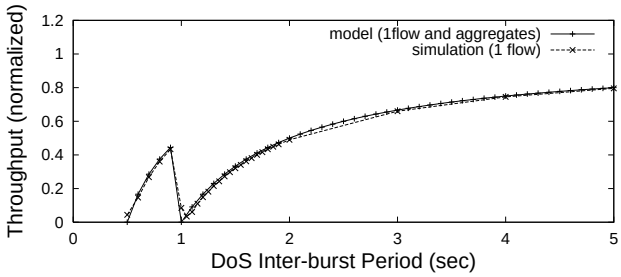

Fig. 4. DoS TCP throughput: model and simulation

Note that the average rate of the DoS attacker is decreasing with increasing T as its average rate is given by Rl/T. However, as indicated by Equation (2) and Figure 4, the effectiveness of the attack is clearly *not* increasing with the attacker's average rate. Most critically, observe that there are two "nulls" in the frequency response in which TCP throughput becomes *zero*. In particular, $\rho(T) = 0$ when $T =$ minRTO and $T =$ minRTO$/2$. The physical interpretation is as follows: if the attacker creates the minRTO-periodic outages, it will completely deny service to the TCP traffic. Once the brief outage occurs, all flows will simultaneously timeout. When their timeout expires after minRTO seconds and they again transmit packets, the attacker creates another outage such that the flows backoff again. Clearly, the most attractive period for a DoS attacker is minRTO (vs. minRTO/2), since it is the null frequency that minimizes the DoS flow's average rate. When $T >$ minRTO, as the period of the attack increases, the TCP flows obtain increasingly higher throughput in periods between expiration of retransmis-

sion timers and the subsequent DoS outage.

Next, we perform a set of *ns* simulations to compare against the model. In these experiments, we again consider the scenario of Figure 3 but with a single TCP flow.[5] The TCP Sack flow has minRTO $= 1$ second and satisfies conditions (C1) and (C2). More precisely, the propagation delay is 6 ms while the buffer size is set such that the round-trip time may vary from 12 ms to 132 ms. The link capacity is 1.5 Mb/s, while the DoS traffic is a square-wave stream with the peak rate 1.5 Mb/s and burst length 150 ms.

The curve labeled "simulation" in Figure 4 depicts the measured normalized throughput of the TCP flow. Figure 4 reveals that Equation (2) captures the basic frequency response of TCP to the shrew DoS attack, characterizing the general trends and approximating the location of the two null frequencies.

IV. Creating DoS Outages

In this section, we explore the traffic patterns that attackers can use in order to create temporary outages that induce recurring TCP timeouts. First, we study the instantaneous bottleneck-queue behavior in periods when an attacker bursts packets into the network. Next, we develop the DoS stream which minimizes the attacker's average rate while ensuring outages of a particular length. Finally, we study square-wave DoS streams and identify the conditions in which they accurately approximate the two-rate DoS streams.

A. Instantaneous Queue Behavior

Consider a bottleneck buffer shared by a TCP flow and a DoS flow which every T seconds bursts at a constant rate R_{DoS} for duration l. Denote R_{TCP} as the instantaneous rate of the TCP flow, B as the buffer size, and B_0 as the buffer size at the onset of an attack, assumed to occur at $t = 0$.

Denote l_1 as the time that the buffer becomes full such that

$$l_1 = \frac{(B - B_0)}{R_{DoS} + R_{TCP} - C}. \quad (3)$$

After l_1 seconds, the buffer remains full for $l_2 = l - l_1$ seconds if $R_{DoS} + R_{TCP} \geq C$. Moreover, if $R_{DoS} \geq C$ during the same period, this will create an outage to the TCP flow whose loss probability will instantaneously increase significantly and force the TCP flow to enter a retransmission timeout with high probability (see also Figure 3).

B. Minimum Packet DoS Streams

Suppose the attacker is limited to a peak rate of $R_{\max}$ due to a secondary bottleneck or the attacker's access link rate. To avoid router-based mechanisms that detect high rate flows, e.g., [26], DoS attackers are interested in ways to minimally expose their streams to detection mechanisms. To minimize the number of bytes transmitted while ensuring outages of a particular length, an attacker should transmit a two-rate DoS stream as depicted in Figure 5. To fill the buffer without help from background traffic or the attacked flow requires $l_1 = B/(R_{\max} - C)$ seconds. Observe that sending at the maximum possible rate $R_{\max}$ minimizes l_1 and consequently the number of required bytes. Once the buffer fills, the attacker should reduce its rate to the bottleneck rate C to ensure continued loss using the lowest possible rate.

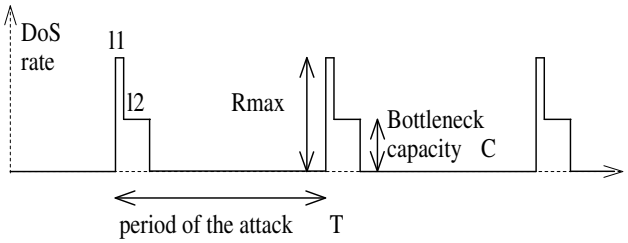

Fig. 5. Two-rate DoS stream

Thus, two-rate streams *minimize* the number of packets that need to be transmitted (for a given bottleneck buffer size B, bottleneck capacity C, and range of sending rates from 0 to $R_{\max}$) among all possible sending streams that are able to ensure periodic outages with period T and length l_2.

To generate two-rate DoS streams in real networks, an attacker can use a number of existing techniques to estimate the bottleneck link capacity [4], [6], [18], [23], [31], bottleneck-bandwidth buffer size [25] and secondary bottleneck rate [30].

Regardless the properties of the above two-rate DoS streams, we consider the simpler square-wave DoS attack shown in Figure 2 as an approximation. First, these streams do not require prior knowledge about the network except the bottleneck rate. Second, they isolate the effect of a single time-scale periodic attack.

To study the effectiveness of the square-wave, we perform simulation experiments to compare the two attacks' frequency responses. As an example, we consider a square-wave DoS stream with peak rate 3.75 Mb/s and burst length $l = 50$ ms and a two-rate stream with $R_{\max}$ = 10 Mb/s. For the two-rate stream, l_1 is computed as $B/(R_{\max} - C)$, while l_2 is determined such that the number of packets sent into the network is the same for both streams. The simulation parameters are the same as previously.

The resulting frequency responses in this example and others (not shown) are nearly identical. Consequently, since square-wave DoS streams accurately approximate the two-rate DoS stream and do not require knowledge of network parameters, we use square-wave DoS streams henceforth in both simulations and Internet experiments.

V. Aggregation and Heterogeneity

In this section, we explore the impact of TCP flow aggregation and heterogeneity on the effectiveness of the shrew attack. First, we experiment with long-lived homogeneous-RTT TCP traffic and explore the DoS stream's ability to synchronize flows. Second, we perform experiments in a heterogeneous RTT environment and explore the effect of RTT-based filtering. Third, we study the impact of DoS streams on links dominated by web traffic. Finally, we evaluate several TCP variants' vulnerability to shrews.

[5] Recall that Equation (2) holds for any number of flows. We simulate TCP aggregates in Section V.

As a baseline topology (and unless otherwise indicated) we consider many TCP Sack flows sharing a single congested link with capacity 1.5 Mb/s as in Figure 3. The one-way *propagation* delay is 6 ms and the buffer size is set such that the *round-trip* time varies from 12 ms to 132 ms. The DoS traffic is a square-wave stream with peak rate 1.5 Mb/s, burst duration 100 ms, and packet size 50 bytes. In all experiments, we generate a FTP/TCP flow in the reverse direction, whose ACK packets multiplex with TCP and DoS packets in the forward direction. For each data point in the figures below, we perform five simulation runs and report averages. Each simulation run lasts 1000 sec. The *ns* code and simulation scripts are available at *http://www.ece.rice.edu/networks/shrew*.

A. Aggregation and Flow Synchronization

The experiments of Section III illustrate that a DoS square wave can severely degrade the throughput of a *single* TCP flow. Here, we investigate the effectiveness of low bit-rate DoS streams on TCP aggregates with homogeneous RTTs for five long-lived TCP flows sharing the bottleneck.

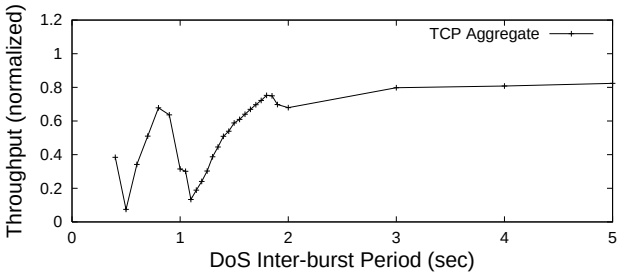

Fig. 6. DoS and aggregated TCP flows

Figure 6 depicts the normalized *aggregate* TCP throughput under the shrew attack for different values of the period T. Observe that similar to the one-flow case, the attack is highly successful so that Equation (2) can also model attacks on aggregates. However, we note that compared to the single-flow case, the throughput at the null 1/minRTO frequency is slightly larger in this case because the maximum RTT of 132 ms is greater than the DoS burst length of 100 ms such that a micro-flow may survive an outage. Also observe that an attack at frequency 2/minRTO nearly completely eliminates the TCP traffic.

The key reasons for this behavior are twofold. First, *RTO homogeneity* (via minRTO) introduces a single vulnerable timescale, even if flows have different RTTs (as explored below). Second, *DoS-induced synchronization* occurs when the DoS outage event causes all flows to enter timeout nearly simultaneously. Together with RTO homogeneity, flows will also attempt to exit timeout nearly simultaneously when they are re-attacked.

Synchronization of TCP flows was extensively explored in [12], [35] and was one of the main motivations for RED [13], whose goal is the avoidance of synchronization of many TCP flows decreasing their window at the same time. In contrast, the approach and scenario here are quite different, as an external malicious source (and not TCP itself) is the source of synchronization. Consequently, mechanisms like RED are unable to prevent DoS-initiated synchronization (see also Section VII).

B. RTT Heterogeneity

B.1 RTT-based Filtering

The above experiment shows that a DoS stream can significantly degrade throughput of a TCP aggregate, provided that the outage length is long enough to force all TCP flows to enter a retransmission timeout simultaneously. Here, we explore a heterogeneous-RTT environment with the objective of showing that a flow's vulnerability to low-rate DoS attacks fundamentally depends on its RTT, with shorter-RTT flows having increased vulnerability.

We perform experiments with 20 long-lived TCP flows on a 10 Mb/s link. The range of round-trip times is 20 to 460 ms [14], obtained from representative Internet measurements [20]. We use these measurements to guide our setting of link propagation delays for different TCP flows.[6]

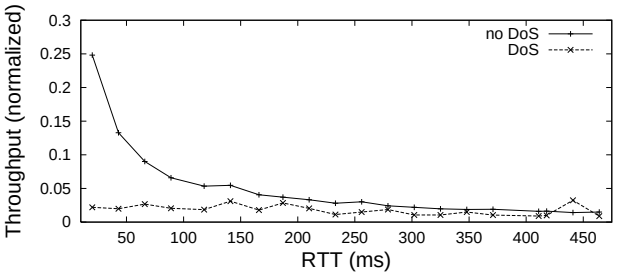

Fig. 7. RTT-based filtering

Figure 7 depicts the normalized TCP throughput for each of the 20 TCP flows. The curve labeled "no DoS" shows each flow's throughput in the absence of an attack. Observe that the flows re-distribute the bandwidth proportionally to 1/RTT such that shorter-RTT flows utilize more bandwidth than the longer ones. The curve labeled "DoS" shows each TCP flow's throughput when they are multiplexed with a DoS square-wave stream with peak rate 10 Mb/s, burst length 100 ms and period 1.1 sec. Observe that this DoS stream filters shorter-RTT flows up to a time-scale of approximately 180 ms, beyond which higher RTT flows are less adversely affected. Also, observe that despite the excess capacity available due to the shrew DoS attack, longer-RTT flows do not manage to improve their throughput.

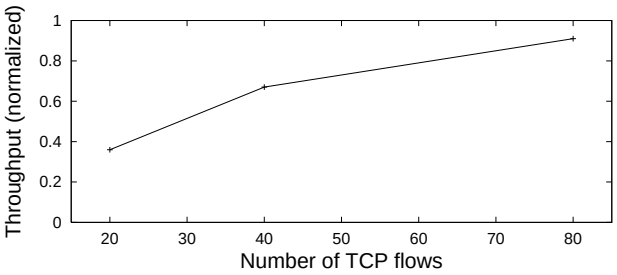

Fig. 8. High aggregation with heterogeneous RTT

However, in a regime with many TCP flows with heterogeneous RTTs, the *number* of non-filtered flows with high RTT

[6] We do not fit the actual CDF of this data, but uniformly distribute round-trip times in the above range.

will increase, and they will eventually be of sufficient number to utilize all available bandwidth left unused by the filtered smaller-RTT flows. Thus, the total TCP throughput will increase with the aggregation level for highly heterogeneous-RTT flows as illustrated in Figure 8. Unfortunately, the high throughput and high link utilization with many flows (e.g., greater than 90% in the 80-flow scenario) is quite misleading, as the shorter-RTT flows have been dramatically rate-limited by the attack as in Figure 7. Hence, one can simultaneously have high utilization and an effective DoS attack against small- to moderate-RTT flows.

B.2 DoS Burst Length

The above experiments showed that DoS streams behave as a high-RTT-pass filter, in which the burst length is related to the filter cut-off time-scale. Here, we directly investigate the impact of burst length.

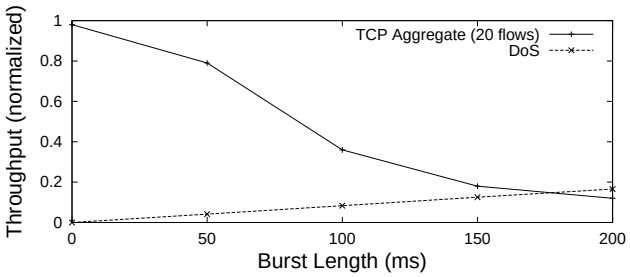

Fig. 9. Impact of DoS burst length

For the same parameters as above, Figure 9 depicts aggregate TCP throughput as a function of the DoS burst length. The figure shows that as the burst length increases, the DoS mean rate increases, yet the aggregate TCP throughput decreases much more significantly. Indeed, as the burst length increases, the RTT-cut-off time-scale increases. In this way, flows with longer and longer RTTs are filtered. Consequently, the number of non-filtered flows decreases such that aggregate TCP throughput decreases. In other words, as the burst length increases, the sub-aggregate for which condition (C1) holds enlarges. With a fixed number of flows, the longer-RTT flows are unable to utilize the available bandwidth, and the aggregate TCP throughput decreases.

B.3 Peak Rate

Recall that the minimal-rate DoS streams studied in Section IV induce outages without any help from background traffic and under the assumption that the initial buffer size B_0 is zero. However, in practice, the buffer will also be occupied by packets from reverse ACK traffic, UDP flows, etc. Consequently, in the presence of such background traffic, the DoS source can potentially lower its peak rate and yet maintain an effective attack.

Consider a scenario with five flows, a DoS flow and four long-lived TCP flows. We set the link propagation delays in the simulator such that one TCP flow experiences shorter RTT (fluctuates from 12 ms to 134 ms) while the other three have longer RTTs (from 108 ms to 230 ms). Figure 10 depicts the throughput of the short-RTT flow as a function of the normalized DoS peak rate varied from 0 to 1. Observe that relatively low peak rates are sufficient to filter the short-RTT flow. For example, a peak

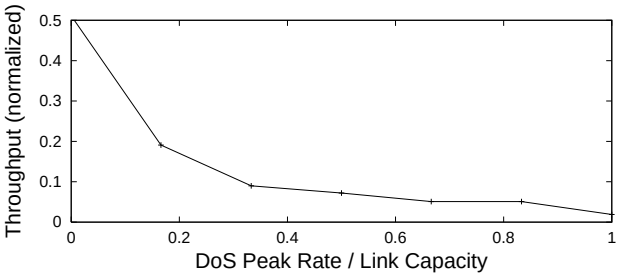

Fig. 10. Impact of DoS peak rate

rate of one third of the link capacity and hence an average rate of 3.3% of the link capacity significantly degrades the short-RTT flows' throughput at the null time-scale. As hypothesized above, longer-RTT flows here play the role of background traffic and increase both B_0 and the burst rate in periods of outages which enables lower-than-bottleneck peak DoS rates to cause outages. This further implies that very low rate periodic flows that operate at one of the null TCP time-scales ($\frac{\text{minRTO}}{j}$, $j = 1, \cdots$) are highly problematic for TCP traffic. For example, some probing schemes periodically burst for short time intervals at high rates in an attempt to estimate the available bandwidth on an end-to-end path [19].

C. HTTP Traffic

Thus far, we have considered long-lived TCP flows. Here, we study a scenario with flow arrival and departure dynamics and highly variable file sizes as incurred with HTTP traffic.

We adopt the model of [10] in which clients initiate sessions from randomly chosen web sites with several web pages downloaded from each site. Each page contains several objects, each of which requires a TCP connection for delivery (i.e., HTTP 1.0). The inter-page and inter-object time distributions are exponential with respective means of 9 sec and 1 msec. Each page consists of ten objects and the object size is distributed according to a Pareto distribution with shape parameter 1.2. For the web transactions, we measure and average the response times for different sized objects.

Figure 11 depicts web-file response times normalized by the response times obtained when the DoS flow is not present in the system. Because of this normalization, the curve labeled "no DoS" in Figure 11 is a straight line with a value of one. The flows' mean HTTP request arrival rate is selected such that the offered HTTP load is 50% and near 100% for Figures 11(a) and 11(b), respectively.

On average, the file response times increased by a factor of 3.5 under 50% load and a factor of 5 under 100% load. Figures 11(a) and 11(b) both indicate that larger files (greater than 100 packets in this scenario) become increasingly and highly vulnerable to the shrew attacks with the response times of files increasing by orders of magnitude. Nevertheless, observe that some flows benefit from the shrew attack and significantly decrease their response times. This occurs when a flow arrives into the system between two outages and manages to transmit its entire file before the next outage occurs.

However, note that this effect is apparent in Figures 11(a) and 11(b) for the longer file sizes, whereas the effect is not observ-

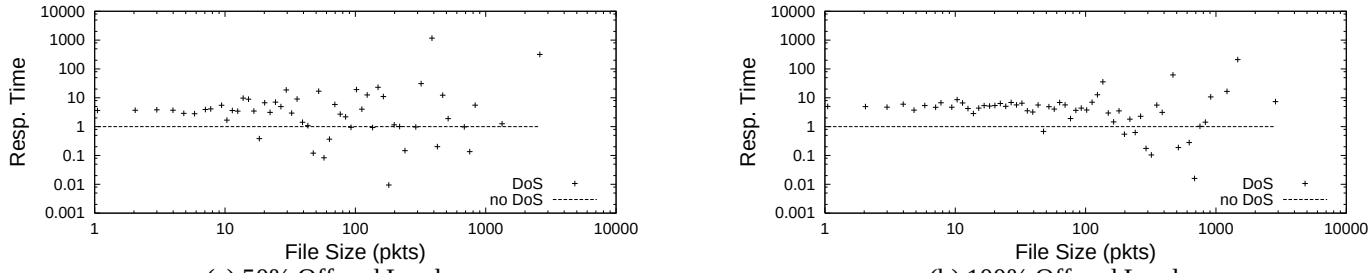

(a) 50% Offered Load (b) 100% Offered Load

Fig. 11. Impact on HTTP flows

able for the shorter file sizes. This is due to the HTTP file-size distribution depicted in Figure 12, which shows that the number of short files is much larger than the number of longer files in a typical web-browsing scenario. Consequently, while many of the short HTTP files actually manage to escape the attack and improve their response times, the response-times *average* is dominantly biased by the flows that are caught by the attack and whose response times are extremely degraded. Thus, while some flows actually benefit from the attack, the overall impact of the shrew attack on HTTP traffic remains quite effective.

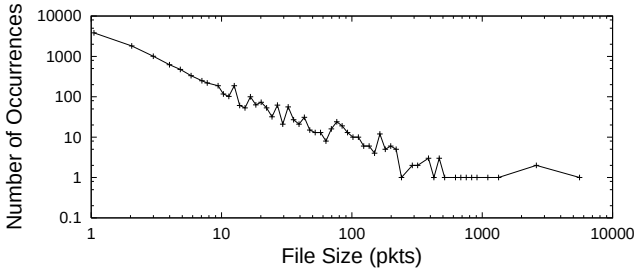

Fig. 12. HTTP file-size distribution

Next, observe that the deviation from the reference (no DoS) scenario is larger in Figure 11(a) than 11(b). This is because the response times are approximately 100 times lower for the no-DoS scenario when the offered load is 50% as compared to the no-DoS scenario when the system is fully utilized.

Finally, we performed experiments where DoS stream attack mixtures of long- (FTP) and short-lived (HTTP) TCP flows. The results (not shown) indicate that the conclusions obtained separately for FTP and HTTP traffic hold for FTP/HTTP aggregates.

D. TCP Variants

The effectiveness of low-rate DoS attacks depends critically on the attacker's ability to create correlated packet losses in the system and force TCP flows to enter retransmission timeout. While we have studied the most robust TCP variant (TCP Sack) so far, many of the existing operating systems today still use some less advanced TCP versions. Here, we first provide a brief background on the work that has been done to build more robust TCP versions and help TCP flows to survive multiple packet losses within a single round-trip time without incurring a retransmission timeout. Then, we evaluate the performance of different TCP versions under the shrew attack.

It is well-known that TCP Reno is the most fragile TCP variant which enters the retransmission timeout whenever a loss happens and less than three duplicate ACKs are received. To overcome this problem, TCP New Reno [16] changes the sender's behavior during Fast Recovery upon receipt of a *partial ACK* that acknowledges some but not all packets that were outstanding at the start of the Fast Recovery period. Further improvements are obtained by TCP Sack [15] when a large number of packets are dropped from a window of data [9] because when a Sack receiver holds non-contiguous data, it sends duplicate ACKs bearing the Sack option to inform the sender of the segments that have been correctly received. A thorough analysis of the packet drops required to force flows of a particular TCP version to enter timeout is given in [9].

Here, we evaluate the performance of TCP Reno, New Reno, Tahoe and Sack under the shrew attack. Figures 13 (a)-(d) show TCP throughput for burst lengths of 30, 50, 70 and 90 ms, respectively. Figure 13(a) confirms that TCP Reno is indeed the most fragile TCP variant, while the other three versions have better robustness to DoS. However, when the peak length increases to 50 ms, *all* TCP variants obtain near zero throughput at the null frequency as shown in Figure 13(b). The Figure also indicates that all TCP variants, including Sack, are the most vulnerable to DoS in the 1 - 1.2 sec time-scale region. During this period, TCP flows are in slow-start and have small window sizes such that a smaller number of packet losses are needed to force them to enter the retransmission timeout. Finally, Figures (c)-(d) indicate that all TCP variations obtain a throughput profile similar to Equation (2) when the outage duration increases, such that more packets are lost from the window of data. Indeed, if all packets from the window are lost, TCP has no alternative but to wait for a retransmission timer to expire.

VI. Internet Experiments

In this section, we describe several DoS experiments performed on the Internet. The scenario is depicted in Figure 14 and consists of a large file downloaded from a TCP Sack sender (TCP-S) to a TCP Sack receiver (TCP-R). While the RFC 2988 [32] recommendation for the minRTO parameter is already in the so-called *should* phase,[7] to the best of our knowledge, it is not yet being widely deployed in the most popular operating systems, which typically set the minRTO parameter to 200 ms. Hence, we configure the TCP-S host to have minRTO $=$ 1 sec (by modifying the Linux-2.4.18 kernel) ac-

[7]The IETF recommendations usually specify the parameter values that (1) *may*, (2) *should*, or (3) *must* be applied.

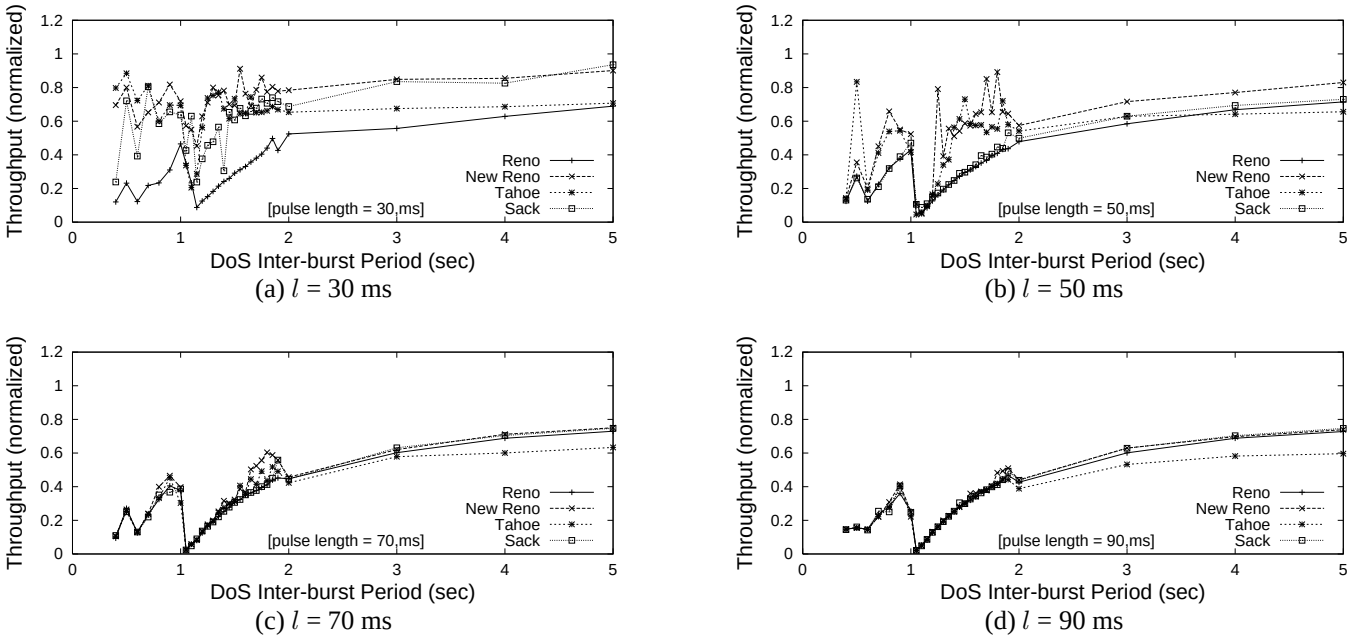

(a) l = 30 ms (b) l = 50 ms

(c) l = 70 ms (d) l = 90 ms

Fig. 13. TCP Reno, New Reno, Tahoe and Sack under shrew attacks

cording to [32], and measure TCP throughput using *iperf*. We launch the shrew attack from three different hosts using a modified version of the UDP-based active probing software from [29] in order to send high-precision DoS streams. We perform three independent measurements for each experiment and report the average results. Both the Linux TCP-kernel source code used in the experiments at the TCP-S side, and the modified UDP-based software used to generate the shrew attacks are available at *http://www.ece.rice.edu/networks/shrew*.

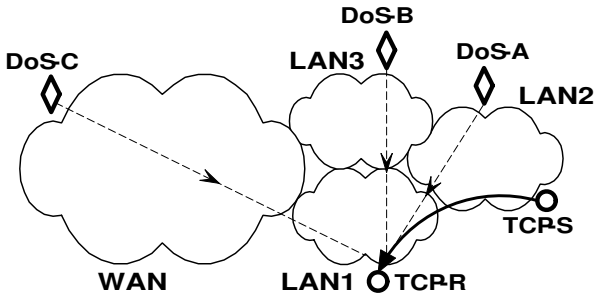

Fig. 14. DoS attack scenario

Intra-LAN Scenario. In this scenario, both the TCP sender (TCP-S) and DoS (DoS-A) hosts are on the same 10 Mb/s Ethernet LAN on Rice University, while the attacked host (TCP-R) is on a different 10 Mb/s Ethernet LAN, two hops away from both TCP-S and DoS-A. The peak rate of the square-wave DoS stream is 10 Mb/s while the burst length is 200 ms. The curve labeled "Intra-LAN" in Figure 15 depicts the results of these experiments. The figure indicates that a null frequency exists at a time-scale of approximately 1.2 sec. When the attacker transmits at this period, it has an average rate of 1.67 Mb/s. Without the DoS stream, the TCP flow obtains 6.6 Mb/s throughput. With it, it obtains 780 kb/s throughput. Thus, the DoS attacker can severely throttle the victim's throughput by nearly an order of magnitude.

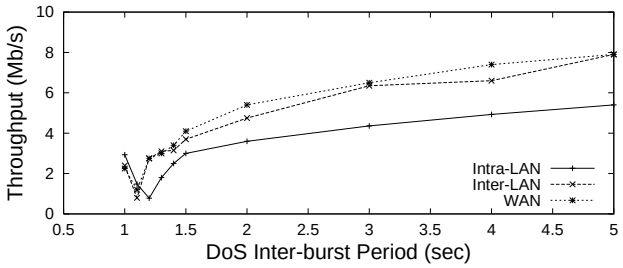

Fig. 15. Internet experiments

Inter-LAN Scenario. In this experiment, the TCP sender (TCP-S), DoS source (DoS-B) and attacked host (TCP-R) are on three different LANs of the ETH (Zurich, Switzerland) campus network. The route between the two traverses two routers and two Ethernet switches, with simple TCP measurements revealing that the TCP and DoS LANs are 100 Mb/s Ethernet LANs, while the attacked host is on a 10 Mb/s Ethernet LAN. The peak rate of the square-wave DoS stream is again 10 Mb/s while its duration is reduced as compared to the Intra-LAN Scenario to 100 ms. The curve labeled "Inter-LAN" in Figure 15 depicts the frequency response of this attack. In this case, a DoS time-scale of $T = 1.1$ sec is the most damaging to TCP, since here the TCP flow achieves 800 kb/s throughput, only 8.1% of the throughput it achieves without DoS flow (9.8 Mb/s). At this time-scale, the attacker has an average rate of 909 kb/s.

WAN Scenario. Finally, for the same TCP source/destination pair as in the Inter-LAN Scenario, source DoS-C initiates a shrew DoS attack from a LAN at EPFL (Lausanne, Switzerland), located eight hops away from the destination. The DoS stream has a peak rate of 10 Mb/s and a burst duration of 100 ms. The curve labeled "WAN" shows the frequency response of these experiments and indicates a nearly identical null located

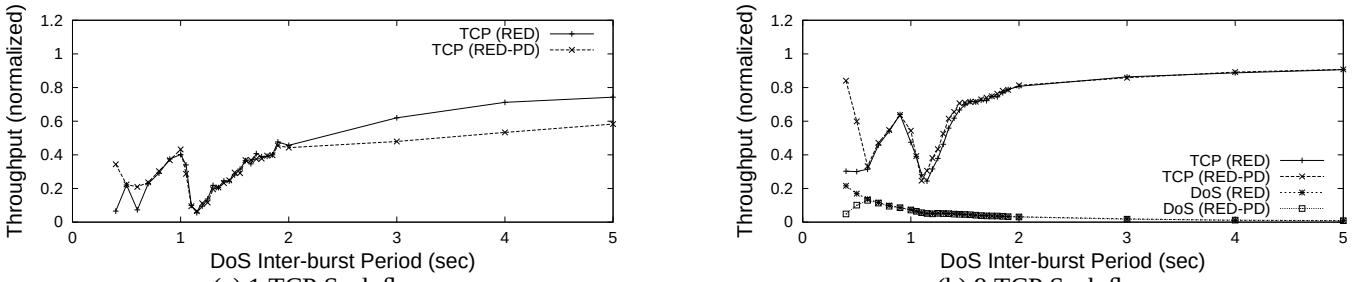

(a) 1 TCP Sack flow (b) 9 TCP Sack flows

Fig. 16. Impact of RED and RED-PD routers

at $T = 1.1$ sec. For this attack, the TCP flow's throughput is degraded to 1.2 Mb/s from 9.8 Mb/s whereas the attacker has average rate of 909 kb/s. This experiment illustrates the feasibility of *remote* attacks. Namely, in the WAN scenario, the DoS attacker has traversed the local provider's network and multiple routers and Ethernet switches before reaching its victim's LAN. Thus, despite potential traffic distortion that deviates the attacker's traffic pattern from the square wave, the attack is highly effective.

Thus, while necessarily small scale due to their (intended) adverse effects, the experiments support the findings of the analytical model and simulation experiments. The results indicate that effective shrew attacks can come from remote sites as well as nearby LANs.

VII. Counter-DoS Techniques

Here, we explore two classes of candidate counter-DoS mechanisms intended to mitigate the effects of shrew attacks: (a) router-assisted, and (b) end-point mechanisms. Out of many router-assisted schemes designed to detect and throttle malicious flows in the network, we focus on the mechanisms that are based on preferential dropping of packets from malicious flows, and evaluate two representatives: RED-PD and CHOKe. From the end-point counter-DoS mechanisms, we first evaluate the effect of the initial TCP congestion window size on the effectiveness of the attack, and then propose and evaluate a counter-DoS mechanism in which end-points randomize their minRTO parameter.

A. Router-Assisted Mechanisms

As described above, DoS flows have low average rate, yet do send relatively high-rate bursts for short time intervals. The key problem lies in the fact that relatively longer time-scales are needed to detect malicious flows with high confidence, while the shrew attack operates on relatively short time-scales. If these shorter time-scales are used to detect malicious flows in the Internet, many legitimate bursty flows would be incorrectly detected as malicious. Here, we investigate if the shrew traffic patterns can be identified as a DoS attack by router-based algorithms.

Mechanisms for per-flow treatment at the router can be classified as scheduling or preferential dropping. Scheduling algorithms place flows in different logical partitions and determine the service rate received by each partition. For example, per-flow Fair Queuing (FQ) scheduling (e.g., [5]) treat each flow as a single partition. While such an approach would completely protect the system against the shrew attack (unless the attacker performs a distributed shrew attack or spoofs packets), per-flow FQ has serious scalability limitations which prevent its deployment. Due to implementation simplicity and other advantages of preferential dropping over scheduling, we focus on dropping algorithms for detection of DoS flows and/or achieving fairness among adaptive and non-adaptive flows. Candidate algorithms include Flow Random Early Detection (FRED) [24], CHOKe [28], Stochastic Fair Blue (SFB) [11], the scheme of reference [3], ERUF [33], Stabilized RED (SRED) [27], dynamic buffer-limiting scheme from [7] and RED with Preferential Dropping (RED-PD) [26]. Of these, we study the most popular representatives: RED-PD and CHOKe.

A.1 RED-PD

RED-PD uses the packet drop history at the router to detect high-bandwidth flows with high confidence. Flows above a configured target bandwidth are identified and monitored by RED-PD. Packets from the monitored flows are dropped with a probability dependent on the excess sending rate of the flow. RED-PD suspends preferential dropping when there is insufficient demand from other traffic in the output queue, for example, when RED's average queue size is less than the minimum threshold.

We perform simulation experiments with one and nine TCP Sack flows, RED-PD routers, and the topology of Figure 3. For one TCP flow, Figure 16(a) indicates that RED-PD is *not* able to detect nor throttle the DoS stream. For aggregated flows depicted in Figure 16(b), RED-PD only affects the system if the attack occurs at a time-scale of less than 0.5 sec, i.e., only unnecessarily high-rate attacks can be addressed. Most critically, at the null time-scale of 1.2 sec, RED-PD has no noticeable effect on throughput as compared to RED. Thus, while RED and RED-PD's randomization has lessened the severity of the null, the shrew attack remains effective overall.

Next, in the above scenario with nine TCP Sack flows, we vary the DoS peak rate and burst length to study the conditions under which the DoS flows will become detectable by RED-PD. We first set the burst duration to 200 ms and then change the peak rate from 0.5 Mb/s to 5 Mb/s. Figure 17(a) indicates that RED-PD starts detecting and throttling the square-wave stream at a peak rate of 4 Mb/s, which is more than twice than the bottleneck rate of 1.5 Mb/s. Recall that in Section V-B.3 we showed that a peak rate of one third the bottleneck capacity and a burst length of 100 ms can be quite dangerous for short-RTT TCP

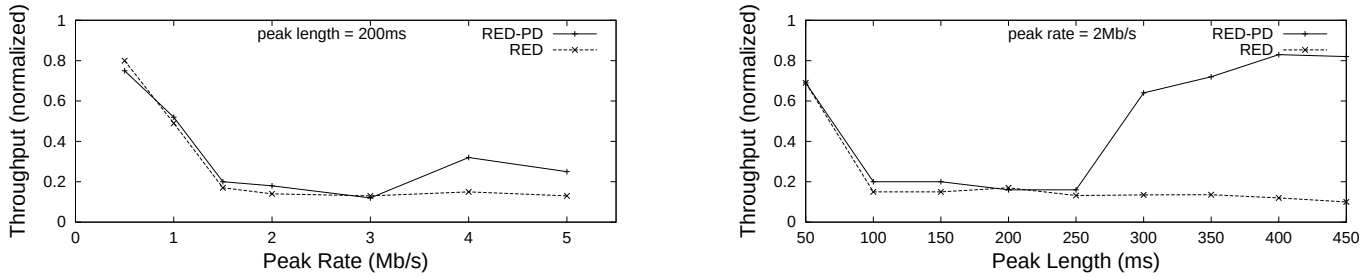

Fig. 17. Detecting DoS streams

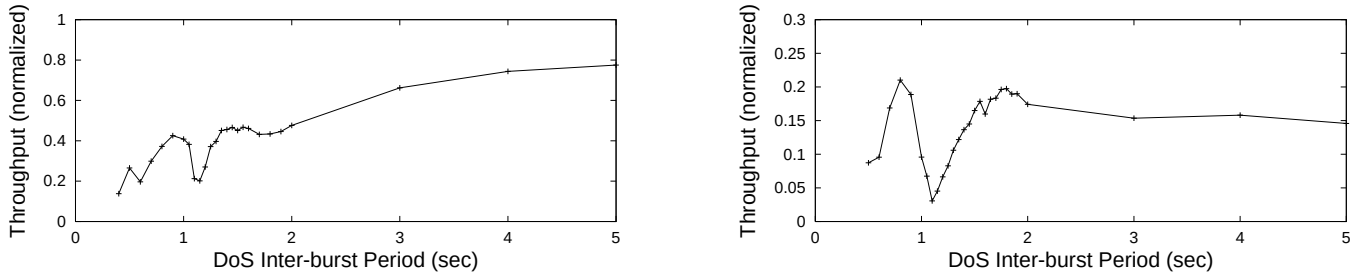

(a) 1 TCP Sack flow (b) Flow filtering

Fig. 18. Impact of CHOKe routers

flows.

Further, we fix the DoS peak rate to 2 Mb/s and vary the burst length from 50 ms to 450 ms. Figure 17(b) shows that RED-PD begins detecting the DoS flow at 300 ms time-scales in this scenario. Recall again that much shorter burst time-scales are sufficient to throttle not only short-RTT flows, but the entire aggregates of heterogeneous-RTT TCP traffic.

Thus, Figure 17(b) captures the fundamental issue of time-scales: RED-PD detects high rate flows on longer time-scales, while DoS streams operate at very short time-scales. If these shorter time-scales are used to detect malicious flows in the Internet, many legitimate bursty TCP flows would be incorrectly detected as malicious. This issue is studied in depth in reference [26], which concludes that long time-scale detection mechanisms are needed to avoid excessively high false positives. However, there are schemes (e.g., [28], [24], [11], [7]) that use very short time-scales to detect high rate flows. While the penalty for their use may be quite h igh, we nevertheless evaluate below the ability of a representative of such schemes (CHOKe) to detect and throttle the shrew attack.

A.2 CHOKe

CHOKe is a dropping scheme designed to throttle unresponsive or misbehaving flows in a congested router. An incoming packet is matched against a random packet in the queue. If they belong to the same flow, both packets are dropped, otherwise the incoming packet is admitted with a certain probability. The scheme tries to leverage the fact that high-bandwidth flows are likely to have more packets in the queue, and tries to approximate fair queuing in a scalable way. While CHOKe is not likely to perform well in high aggregation regimes [26], and despite the indication that the penalty for the use of the scheme may be quite high (especially in low-aggregation regimes and HTTP scenarios), our main goal here is to evaluate its ability to detect the shrew attacks.

We initially perform a simulation experiment with one TCP Sack flow under the shrew attack, CHOKe router, and the topology of Figure 3. Figure 18(a) indicates that CHOKe outperforms RED-PD (compare Figures 16(a) and 18(a)) in thwarting the shrew attacks. This is exactly due to fact that CHOKe operates on much shorter time-scales: it observes instantaneous queue behavior (and not the drop history), and is thus able to mitigate the effectiveness of the attack more successfully. However, observe that CHOKe in this scenario does not completely eliminate the effectiveness of the attack, but only smooths the throughput "dip" on the minRTO time-scale. Finally, as the number of flows increases, CHOKe (like RED-PD) becomes more and more successful in smoothing the TCP aggregate null frequencies (not shown).

However, recall that in Section V-B.3, we showed that in heterogeneous-RTT environments, the shrews are able to deny service to a subset of short-RTT TCP flows, yet *without* bursting at high instantaneous rates. Consequently, the attacker packets *do not* monopolize the buffer resources, and are thus hard to detect. We evaluate this hypothesis below.

Here, we repeat the experiment from Section V-B.3 with a CHOKe router, to evaluate its ability to thwart the shrew attack in the flow-filtering scenario. The experiment consists of an aggregate of long-RTT TCP flows multiplexed with a short-RTT TCP flow. Figure 18(b) depicts the throughput of the short-RTT flow as a function of the shrew inter-burst period, where the peak of the shrew burst is kept to only 1/3 of the bottleneck link capacity. Observe that CHOKe fails to throttle the shrew flow, because this malicious flow is hidden in the aggregate of legitimate long-RTT TCP flows that are not significantly affected by the attack. Thus, while the shrew flow creates periodic outages and denies service to short-RTT flows, it actually never monopolizes the buffer resources, and remains undetected

by the CHOKe router.

B. End-point Mechanisms

Here, we evaluate end-point-based counter-DoS mechanisms. The key idea is to make TCP more robust to shrew attacks by applying a more careful (DoS-resilient) protocol design. We explore two modifications of the existing TCP parameters. The first is the increase of the initial window size parameter; and the second is the randomization of the minRTO parameter.

B.1 Increasing the Initial Window Size

The above experiments indicate that TCP flows are the most vulnerable to shrew attacks when they have small window sizes, simply due to fact that a smaller number of packet losses are needed to force them to enter the retransmission timeout. Here, we explore if increasing the window size after exiting the retransmission timeout (popularly known as "jump-starting" a TCP flow) may help in mitigating the effectiveness of the attack.

The parameter of interest here is the initial window size *W*. The default is two segments, whereas RFC 2414 [1] recommends increasing this parameter to a value between two and four segments (roughly 4 kbytes) to achieve a performance improvement. We perform a number of experiments with TCP flows (with $W = 4$) under the shrew attack, but do not observe any noticeable improvement in such scenarios. While increasing the initial window size parameter beyond four segments may lead to a congestion collapse [1], we nevertheless perform experiments with $W = 8$ and $W = 16$ (not shown), for the sake of research curiosity. The only noticeable difference is that the TCP null time scale slightly moves closer to 1 sec. This happens because a "jump-started" TCP flow utilizes the available bandwidth much faster, but unfortunately the vulnerability to low-rate attacks remains. In summary, as long as the outage length is on the time scale of the flow's RTT, the increased number of packets in flight doesn't help in preventing the attack.

B.2 End-point minRTO Randomization

Since low-rate attacks exploit minRTO homogeneity, we explore a counter-DoS mechanism in which end-points randomize their minRTO parameter in order to randomize their null frequencies. Here, we develop a simple, yet illustrative model of TCP throughput under such a scenario. In particular, we consider a counter-DoS strategy in which TCP senders randomize their minRTO parameters according to a uniform distribution in the range $[a, b]$. Our objective is to compute the TCP frequency response for a single flow with a uniformly distributed minRTO. Moreover, some operating systems use a simple periodic timer interrupt of 500 ms to check for timed-out connections. This implies that while the TCP flows enter timeout at the same time, they recover uniformly over the $[1, 1.5]$ sec range. Thus, the following analysis applies equally to such scenarios.

We have three cases according to the value of T as compared to a and b. First, if $T \geq b$. Then $\rho(T) = \frac{T - E(RTO)}{T}$, where $E(RTO) = (a + b)/2$ so that

$$\rho(T) = \frac{T - \frac{a+b}{2}}{T}, \text{for } T \geq b. \tag{4}$$

Second, for $T \in [a, b)$, denote k as $\lfloor \frac{b}{T} \rfloor$. Then,

$$\rho(T) = \frac{T-a}{b-a}\frac{T - \frac{T+a}{2}}{T} + \sum_{i=1}^{k-1} \frac{T}{b-a}\frac{\frac{T}{2}}{(i+1)T} + \frac{b-kT}{b-a}\frac{(k+1)T - \frac{kT+b}{2}}{(k+1)T}. \tag{5}$$

Equation (5) is derived as follows. Since only one outage at a time can cause a TCP flow to enter retransmission timeout, we first determine the probability for each outage to cause a retransmission timeout and then multiply it by the corresponding conditional expectation for the TCP throughput. In Equation (5), the first term denotes TCP throughput in the scenario when the retransmission timeout is caused by the next outage after the initial one. The term $\frac{T-a}{b-a}$ denotes the probability that the initial RTO period has expired, which further means that the first outage after time a will cause another RTO. The conditional expectation for TCP throughput in this scenario is $\frac{T - \frac{T+a}{2}}{T}$, where $\frac{T+a}{2}$ denotes the expected value of the end of the initial RTO, given that it happened between a and T. The second term of Equation (5) denotes TCP throughput for outages $i = 2, \cdots, k-1$. The probability for them to occur is $\frac{T}{b-a}$, and the conditional expectation of TCP throughput is $\frac{T/2}{(i+1)T}$. Finally, the third term in Equation (5) denotes TCP throughput for the $(k+1)^{th}$ outage.

Finally, when $T < a$, it can be similarly shown that

$$\rho(T) = \frac{\lceil \frac{a}{T} \rceil T - \frac{a+b}{2}}{\lceil \frac{a}{T} \rceil T}, \text{for } k = 1, \tag{6}$$

and

$$\rho(T) = \frac{\lceil \frac{a}{T} \rceil T - a}{b-a}\frac{\lceil \frac{a}{T} \rceil T - \frac{a + \lceil \frac{a}{T} \rceil T}{2}}{\lceil \frac{a}{T} \rceil T} + \sum_{i=\lceil \frac{a}{T} \rceil}^{k-1} \frac{T}{b-a}\frac{\frac{T}{2}}{(i+1)T} + \frac{b-kT}{b-a}\frac{(k+1)T - \frac{kT+b}{2}}{(k+1)T}, \text{for } k \geq 2. \tag{7}$$

Figure 19 shows that the above model matches well with simulations for minRTO = uniform$(1, 1.2)$. Observe that randomizing the minRTO parameter shifts both null time scales and amplitudes of TCP throughput on these time-scales as a function of a and b. The longest most vulnerable time-scale now becomes $T = b$. Thus, in order to minimize the TCP throughput, an attacker should wait for the retransmission timer to expire, and then create an outage. Otherwise, if the outage is performed prior to b, there is a probability that some flows' retransmission timers have not yet expired. In this scenario, those flows survive the outage and utilize the available bandwidth until they are throttled by the next outage.

Because an attacker's ideal period is $T = b$ under minRTO randomization, we present the following relationship between aggregate TCP throughput and the DoS time-scale.

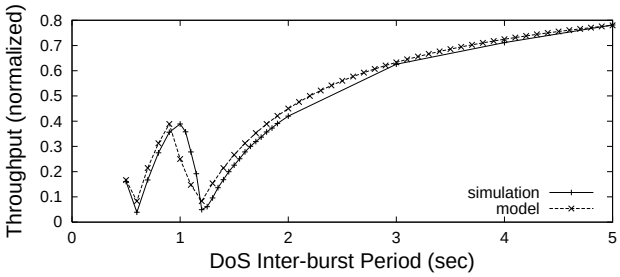

Fig. 19. DoS under randomized RTO

Counter-DoS Randomization Result. *Consider n long-lived TCP flows that experience b-periodic outages. The normalized* aggregate *throughput of the n flows is approximately*

$$\rho(T=b) = \frac{b-(a+\frac{b-a}{n+1})}{b} \tag{8}$$

The derivation is given in the Appendix.

Equation (8) indicates that as the number of flows n increases, the normalized aggregate TCP throughput in the presence of $T = b$ time-scale DoS attacks converges toward $\frac{b-a}{b}$. Indeed, consider the case that all flows experience an outage at the same reference time zero. When the number of flows in the system is high, a fraction of flows' retransmission timers will expire sufficiently near time a such that those flows can partially recover and utilize the available bandwidth in the period from time a to time b, when all flows will again experience an outage. For the scenario of operating systems that use a 500 ms periodic timeout interrupt, such that a flow "times out" uniformly in a [1,1.5] range, Equation (8) indicates that the TCP throughput degrades from 0.17 (a single TCP flow) to 0.34 (TCP aggregate with many flows) under the 1.5 sec periodic attack.

There are two apparent strategies for increasing throughput on $T = b$ time-scales. First, it appears attractive to decrease a which would significantly increase TCP throughput. Alternatively, decreasing both a and b would force the attacker to send very close bursts, making it no longer a stealthy attack. However, recall that conservative timeout mechanisms are fundamentally required to achieve high performance during periods of heavy congestion [2]. Second, while increasing b also increases TCP throughput, it does so only in higher aggregation regimes (when n is sufficiently large) and in scenarios with long-lived TCP flows. On the other hand, increasing b is not a good option for low aggregation regimes (when n is small) since the TCP throughput can become too low since we have $\rho(T = b) = \frac{n}{n+1}\frac{b-a}{b}$. Moreover, excessively large b could significantly degrade the throughput of short-lived HTTP flows which form the majority traffic in today's Internet. In summary, minRTO randomization indeed shifts and smooths TCP's null frequencies. However, as a consequence of RTT heterogeneity, the fundamental tradeoff between TCP performance and vulnerability to low-rate DoS attacks remains.

VIII. Conclusions

This paper presents denial of service attacks that are able to throttle TCP flows to a small fraction of their ideal rate while transmitting at sufficiently low average rate to elude detection. We showed that by exploiting TCP's retransmission timeout mechanism, TCP exhibits null frequencies when multiplexed with a maliciously chosen periodic DoS stream. We developed several DoS traffic patterns (including the minimum rate one) and through a combination of analytical modeling, an extensive set of simulations, and Internet experiments we showed that (1) low-rate DoS attacks are successful against both short- and long-lived TCP aggregates and thus represent a realistic threat to today's Internet; (2) in a heterogeneous-RTT environment, the success of the attack is weighted towards shorter-RTT flows; (3) low-rate periodic open-loop streams, even if not maliciously generated, can be very harmful to short-RTT TCP traffic if their period matches one of the null TCP frequencies; and (4) both network-router and end-point-based mechanisms can only mitigate, but not eliminate the effectiveness of the attack.

The underlying vulnerability is not due to poor design of DoS detection or TCP timeout mechanisms, but rather to an inherent tradeoff induced by a mismatch of defense and attack timescales. Consequently, to completely defend the system in the presence of such attacks, one would necessarily have to significantly sacrifice system performance in their absence.

Acknowledgments

We thank Roger Karrer (Rice University) for help in obtaining accounts at ETH and EPFL, Luca Previtali and Matteo Corti (ETH's Lab of Software Technology) for providing the hardware and software for the Internet experiments, Peter Bircher and Armin Brunner (responsible for network security at ETH), for allowing the experiments, and Martin Vitterli (EPFL) for providing a computer account. Next, we thank Attila Pasztor and Darryl Veitch (University of Melbourne) for sharing their active probing software to perform the Internet experiments. Finally, we thank the anonymous reviewers of [22], whose ideas, suggestions, and critics are built in this paper.

References

[1] M. Allman, S. Floyd, and C. Partridge. Increasing TCP's initial window, 1998. Internet RFC 2414.

[2] M. Allman and V. Paxson. On estimating end-to-end network path properties. In *Proceedings of ACM SIGCOMM '99*, Vancouver, British Columbia, September 1999.

[3] F. Anjum and L. Tassiulas. Fair bandwidth sharing among adaptive and non-adaptive flows in the Internet. In *Proceedings of IEEE INFOCOM '99*, New York, NY, March 1999.

[4] R. L. Carter and M. E. Crovella. Measuring bottleneck link speed in packet-switched networks. *Performence Evaluation*, 27(28):297–318, 1996.

[5] Alan Demers, Srinivasan Keshav, and Scott Shenker. Analysis and simulation of a fair queueing algorithm. In *Journal of Internetworking Research and Experience*, volume 1, pages 3–26, September 1990.

[6] C. Dovrolis, P. Ramanathan, and D. Moore. What do packet dispersion techniques measure? In *Proceedings of IEEE INFOCOM '01*, Anchorage, Alaska, April 2001.

[7] F. Ertemalp, D. Chiriton, and A. Bechtolsheim. Using dynamic buffer limiting to protect against belligerent flows in high-speed networks. In *Proceedings of IEEE ICNP '01*, Riverside, CA, November 2001.

[8] C. Estan and G. Varghese. New directions in traffic measurement and accounting. In *Proceedings of ACM SIGCOMM '02*, Pittsburgh, PA, Aug. 2002.

[9] K. Fall and S. Floyd. Simulation-based comparison of Tahoe, Reno and SACK TCP. *ACM Computer Comm. Review*, 5(3):5–21, July 1996.

[10] A. Feldmann, A. Gilbert, P. Huang, and W. Willinger. Dynamics of IP traffic: A study of the role of variability and the impact of control. In *Proceedings of ACM SIGCOMM '99*, Vancouver, British Columbia, September 1999.

[11] W. Feng, D. Kandlur, D. Saha, and K. Shin. Stochastic fair BLUE: A queue management algorithm for enforcing fairness. In *Proceedings of IEEE INFOCOM '01*, Anchorage, Alaska, June 2001.

[12] S. Floyd and V. Jacobson. On traffic phase effects in packet-switched gateways. *Internetworking: Research and Experience*, 3(3):115–156, September 1992.

[13] S. Floyd and V. Jacobson. Random early detection gateways for congestion avoidance. *IEEE/ACM Transactions on Networking*, 1(4):397–413, 1993.

[14] S. Floyd and E. Kohler. Internet research needs better models. In *Proceedings of HOTNETS '02*, Princeton, New Jersey, October 2002.

[15] S. Floyd, J. Madhavi, M. Mathis, and M. Podolsky. An extension to the selective acknowledgement (SACK) option for TCP, July 2000. Internet RFC 2883.

[16] J. Hoe. Improving the start-up behavior of a congestion control scheme for TCP. In *Proceedings of ACM SIGCOMM '96*, Stanford University, CA, August 1996.

[17] V. Jacobson. Congestion avoidance and control. *ACM Computer Comm. Review*, 18(4):314–329, Aug. 1988.

[18] V. Jacobson. Pathchar: A tool to infer characteristics of Internet paths. *ftp://ftp.ee.lbl.gov/pathchar/*, Apr. 1997.

[19] M. Jain and C. Dovrolis. End-to-end available bandwidth: Measurement methodology, dynamics, and relation with TCP throughput. In *Proceedings of ACM SIGCOMM '02*, Pittsburgh, PA, Aug. 2002.

[20] H. Jiang and C. Dovrolis. Passive estimation of TCP round-trip times. *ACM Computer Comm. Review*, 32(3):5–21, July 2002.

[21] P. Karn and C. Partridge. Improving round-trip time estimates in reliable transport protocol. *ACM Transactions on Computer Systems*, 9(4):364–373, November 1991.

[22] A. Kuzmanovic and E. Knightly. Low-rate TCP-targeted denial of service attacks (the shrew vs. the mice and elephants). In *Proceedings of ACM SIGCOMM '03*, Karlsruhe, Germany, August 2003.

[23] K. Lai and M. Baker. Measuring link bandwidths using a deterministic model of packet delay. In *Proceedings of ACM SIGCOMM '00*, Stockholm, Sweden, August 2000.

[24] D. Lin and R. Morris. Dynamics of Random Early Detection. In *Proceedings of ACM SIGCOMM '97*, Cannes, France, September 1997.

[25] J. Liu and M. Crovella. Using loss pairs to discover network properties. In *Proceedings of IEEE/ACM SIGCOMM Internet Measurement Workshop*, San Francisco, CA, Nov. 2001.

[26] R. Mahajan, S. Floyd, and D. Wetherall. Controlling high-bandwidth flows at the congested router. In *Proceedings of IEEE ICNP '01*, Riverside, CA, November 2001.

[27] T. J. Ott, T. V. Lakshman, and L. Wong. SRED: Stabilized RED. In *Proceedings of IEEE INFOCOM '99*, New York, NY, March 1999.

[28] R. Pain, B. Prabhakar, and K. Psounis. CHOKe, a stateless active queue management scheme for approximating fair bandwidth allocation. In *Proceedings of IEEE INFOCOM '00*, Tel Aviv, Israel, March 2000.

[29] A. Pasztor and D. Veitch. High precision active probing for Internet measurement. In *Proceedings of INET '01*, Stockholm, Sweden, 2001.

[30] A. Pasztor and D. Veitch. The packet size dependence of packet pair like methods. In *Proceedings of IWQoS '02*, Miami, FL, May 2002.

[31] V. Paxson. End-to-end Internet packet dynamics. *IEEE/ACM Transactions on Networking*, 7(3):277–292, June 1999.

[32] V. Paxson and M. Allman. Computing TCP's retransmission timer, November 2000. Internet RFC 2988.

[33] A. Rangarajan and A. Acharya. ERUF: Early regulation of unresponsive best-effort traffic. In *Proceedings of IEEE ICNP '99*, Toronto, CA, October 1999.

[34] A. C. Snoeren, C. Partridge, L. A. Sanchez, C. E. Jones, F. Tchakountio, S. T. Kent, and W. T. Strayer. Hash-based IP traceback. In *Proceedings of ACM SIGCOMM '01*, San Diego, CA, August 2001.

[35] L. Zhang, S. Shenker, and D. Clark. Observation on the dynamics of a congestion control algorithm: The effects of two-way traffic. In *Proceedings of ACM SIGCOMM'91*, Zurich, Switzerland, September 1991.

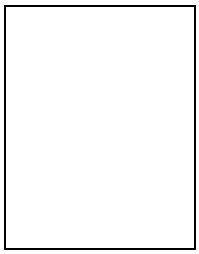

Aleksandar Kuzmanovic is an assistant professor in the Department of Electrical Engineering and Computer Science at Northwestern University. He received his B.S. and M.S. degrees from the University of Belgrade, Serbia, in 1996 and 1999 respectively. He received the Ph.D. degree from the Rice University in 2004. His research interests are in the area of computer networking with emphasis on design, security, analysis, theory, and prototype implementation of protocols and algorithms for the wired and wireless Internet.

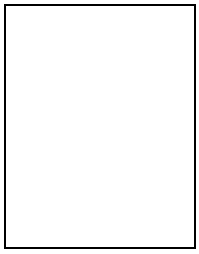

Edward W. Knightly (SM '04) is an associate professor of Electrical and Computer Engineering at Rice University. He received the B.S. degree from Auburn University in 1991 and the M.S. and Ph.D. degrees from the University of California at Berkeley in 1992 and 1996 respectively. He is an associate editor of IEEE/ACM Transactions on Networking. He served as technical co-chair of IEEE IWQoS 1998 and IEEE INFOCOM 2005 and served on the program committee for numerous networking conferences including ICNP, INFOCOM, IWQoS, MobiCom, and SIGMETRICS. He received the National Science Foundation CAREER Award in 1997 and the Sloan Fellowship in 2001. His research interests are in the areas of mobile and wireless networks and high-performance and denial-of-service resilient protocol design.

APPENDIX

Computing the throughput of a TCP aggregate on the $T = b$ time-scale.

Assume that an initial outage causes all TCP flows to enter the retransmission timeout and assume that $T = b$. Then, the throughput of the TCP aggregate can be computed as

$$\rho(T = b) = \frac{b - E(x)}{b}, \tag{9}$$

where $E(X)$ denotes expected value of a random variable X which corresponds to an event that at least one TCP flow's timeout expired at time x, $x \in [a, b]$. Assuming that each TCP flow's minRTO is uniformly distributed between a and b, the CDF of X becomes

$$P(X \leq x) = 1 - (\frac{b - x}{b - a})^n. \tag{10}$$

Denoting the corresponding pdf of random variable X as $p(x)$, we have

$$p(x) = \frac{\partial P(X \leq x)}{\partial x} = n\frac{(b - x)^{n-1}}{(b - a)^n}. \tag{11}$$

The expected value of X, $E(X)$ can be computed as

$$E(X) = \int_a^b xn\frac{(b - x)^{n-1}}{(b - a)^n}\, dx. \tag{12}$$

The integral from Equation (12) can be solved by using integration by parts with the substitutes $n\frac{(b-x)^{n-1}}{(b-a)^n} = dv$ and $x = u$. The solution is $E(X) = a + \frac{b-a}{n+1}$. Thus, based on Equation (9), we have that Equation (8) holds.